A Tri-Band Antenna for Wireless Applications using Slot-Type SRR

D.-L. Jin, T.-T. Bu, J.-S. Hong, J.-F. Wang, and H. Xiong

School of Physical Electronics
University of Electronic Science and Technology, Chengdu, 610054, China
jindalinyu@163.com, butingting1990@gmail.com, cemlab@uestc.edu.cn, 773882005@qq.com,
xiong1226han@126.com

Abstract ─ A tri-band microstrip-fed slot antenna for WLAN/WiMAX applications is proposed and investigated. Three operating bands are obtained by inserting split ring resonator (SRR) slots for band-rejected design. An electromagnetic (EM) model of this antenna is simulated by Ansoft HFSS. The principle of operation and parametric of the proposed antenna are also provided. The measured -10 dB bandwidth for return loss is from 2.39 GHz – 2.48 GHz, 3 GHz – 3.7 GHz, and 5 GHz – 7 GHz, covering the WLAN (2.4/5.2/5.8) and WiMAX (3.5/5.5) bands. The proposed antenna achieves a stably omni-directional radiation pattern and acceptable gain at all three operating frequency bands.

Index Terms – Slot antennas, SRR, tri-band antennas, and WiMAX/WLAN applications.

I. INTRODUCTION

With the rapid development of the wireless communication, the multiband antennas have great interest for the application to communication systems. A printed monopole antenna is very attractive and suitable for the multiband WLAN/WiMAX applications owing to their simple structures, low profile, good impedance matching, low cost, and omni-directional radiation patterns [1-17]. Numerous monopole designs have been investigated for wireless systems. Multiband monopole antenna can be realized by employing a parasitic or shorted element to the monopole antenna [1-4], appropriately etching slots in radiating elements [8-10], using various radiating elements of different shapes [11-13] and various feeding structure[15-17].

However, the first method will increase the manufacturing cost and difficulty in fabricating. Most of the reported multiband antennas combine the last three method have either large antenna sizes or complex structures. In [18], a triple-band unidirectional coplanar antenna with high gain and good impedance matching is proposed for WLAN/WiMAX applications, but the size is 100×60 mm^2. A CPW-fed mirrored-L monopole antenna has distinct triple-band, but the geometry of the antenna is complicated and the size (77×53 mm^2) is relatively large [19].

In this paper, a novel triple band planar monopole antenna with complementary split ring resonators (SRR) is proposed. The antenna is simple in structure and reduced the size compared to the conventional printed monopole antenna. By embedding different shaped SRR slots into a rectangular patch [20] for band-rejected design, a triple-band antenna with compact size, low profile, good radiation performance, and without conductor-backed plane is obtained. From the measured results, the impedance bandwidth for -10 dB return loss at 2.44 GHz, 3.5 GHz, 5.5 GHz operating bands can be respectively up to 0.09 GHz, 0.7 GHz, and 2 GHz. The proposed antenna is suitable for multiband wireless communication systems such as the wireless local-area network (WLAN) 2.4/5.2/5.8 and the world interoperability for microwave access (WiMAX) 3.5/5.5 operations owing to its omni-directional radiation patterns and good impedance characteristics.

II. ANTENNA DESIGN

Figure 1 shows the geometry of the proposed multiband antenna. The antenna is printed on 1.2 mm thick FR4 substrate of relative permittivity 4.4

Submitted On: Dec. 26, 2012
Accepted On: Feb. 2, 2014

with overall dimensions of 26×32 mm^2. The radiation element of the triple band antenna simply composed of a rectangular monopole with SRR slots and 50 Ω microstrip feeding line is printed on the top side of substrate. The width (W_1) and length (L_1) of the microstrip feed line is designed as 2.2 mm to achieve the 50 Ω characteristic impedance. Figure 2 illustrated the photograph of the fabricated antenna. For detailed design, all parameters of the proposed antenna are simulated and optimized using the Ansoft HFSS in finite-element moment based full-wave solver.

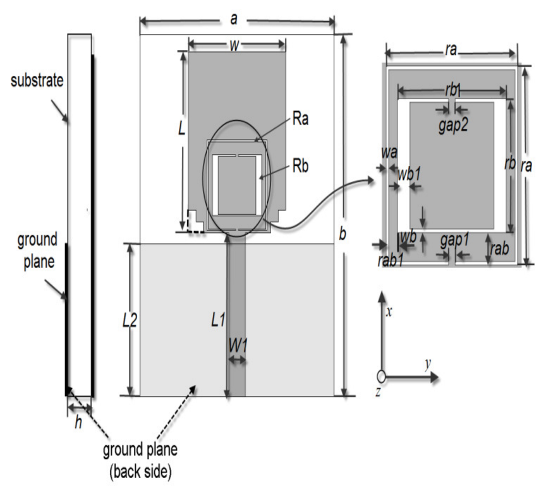

Fig. 1. Geometry of the proposed antenna.

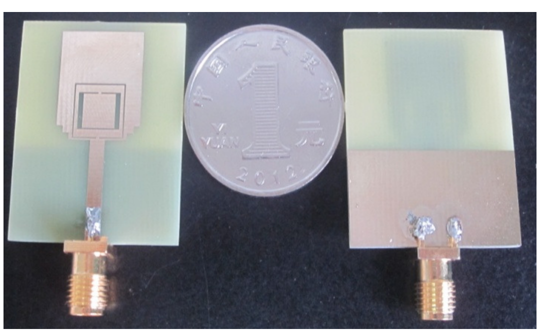

Fig. 2. Photograph of the proposed triple band antenna.

The dimensions of the designed antenna after optimization are: a = 26 mm, b = 32 mm, W = 13 mm, L = 16 mm, W_1 = 2.2 mm, L_1 = 14.5 mm, L_2 = 13.5 mm, ra = 8 mm, rb = 5.4 mm, $rb1$ = 6.6 mm, rab = 1.1 mm, $rab1$ = 0.5 mm, $gap1$ = $gap2$ = 0.4 mm, wa = wb = 0.2 mm, $wb1$ = 0.8 mm. As shown in Fig. 3, the initial antenna has a wide bandwidth from 3.1 GHz − 7 GHz, and the performance beyond 7 GHz is out of our interest for WLAN/WiMAX applications. It also can be seen from the figure that the inner split ring (*Rb*) is for notched the 3.8 GHz − 4.9 GHz and the lower band at 2.44 GHz is attributed to the outer split ring (*Ra*). Then the final triple band antenna for wireless applications is obtained by combined the inner and outer split ring. The detail performance of the SRR will be given as the following.

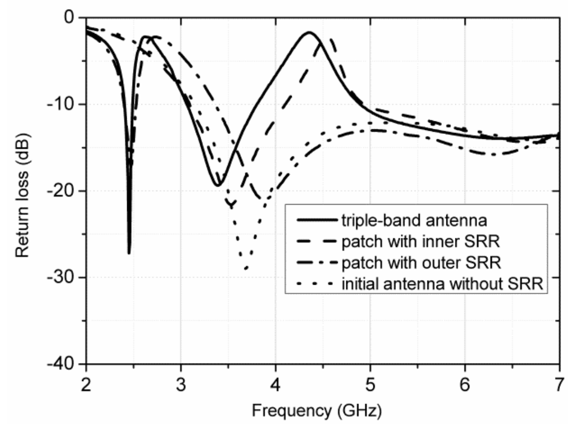

Fig. 3. Simulated return losses for the different structures.

A. The inner split ring inserting

The initial wideband antenna has a bandwidth from 3.1 GHz to 7 GHz as shown in Fig. 3. From Fig. 4 (a), it can be seen that the initial wideband monopole antenna consists of a regular rectangle patch and ground plane, while the staircase pattern is used to broadband, because the electromagnetic coupling between the rectangular patch and the ground plane is affected by the two staircase pattern notches [21-23]. In order to reduce the EMI, band-notched function covering the 3.8 GHz – 4.9 GHz is desired. The band-notched (3.8 GHz – 4.9 GHz) antenna is illustrated in Fig. 4 (c). As shown in Fig. 5, *wb1* is an important parameter to broad the notched band. The notched band is extended to 4.9 GHz, while *wb1* change from 0.2 mm to 0.8 mm. The inner split ring (*Rb*) is designed to get the notched band. The simulated current distribution of the wideband antenna at the notched frequency 4.4 GHz is shown in Fig. 6. Note that the currents are manly distributed around the SRR filter structure. The length of SRR slots is determined by,

$$Ls = \frac{\lambda_g}{2} = \frac{\lambda_0}{2\sqrt{\varepsilon_e}} = \frac{c}{2\sqrt{\varepsilon_e} f_0} \qquad (1)$$

where f_0 is the band-notch frequency (4.4 GHz), $\varepsilon_e = (\varepsilon_r + 1)/2$, is the effective dielectric constant, and c is the speed of light in free space. The inner SRR leads to the desired notch frequency at 4.4 GHz (3.8 GHz – 4.9 GHz), and the length *Ls* = 21.6 mm is about half of the guided wavelength (λg/2) calculated at 4.4 GHz.

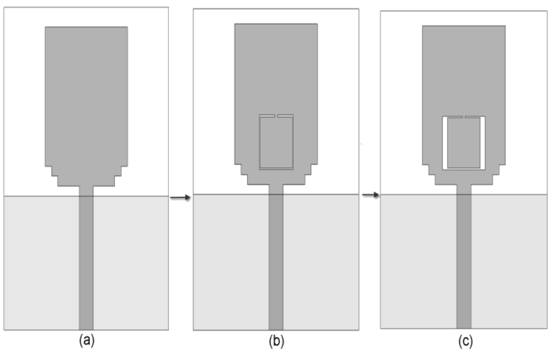

Fig. 4. (a) Initial monopole antenna, (b) band-notched antenna with inner split ring inserting (*wb1* = 0.2 mm), and (c) band-notched antenna with inner split ring inserting (*wb1* = 0.8 mm).

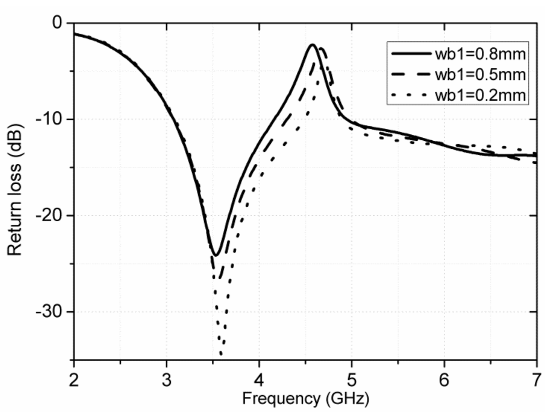

Fig. 5. Simulated return loss for different *wb1*.

Parameters *rb1* and *gap2* are varied with a range of values also as part of the optimization process. As shown in Fig. 7, the notched band shifts to higher frequency as *rb1* and *gap2* increase. As *rb1* and *gap2* gradually increased to 6.6 mm and 0.4 mm, a good impedance match is achieved and the notched antenna can be suitable for reduce EMI with the higher band (3.8 GHz – 4.9 GHz), and the wideband antenna is adjusted to dual band antenna.

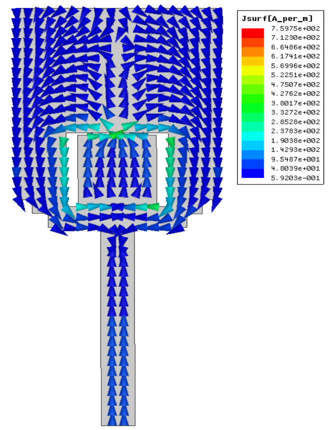

Fig. 6. The surface current distribution at this rejection frequency (4.4 GHz).

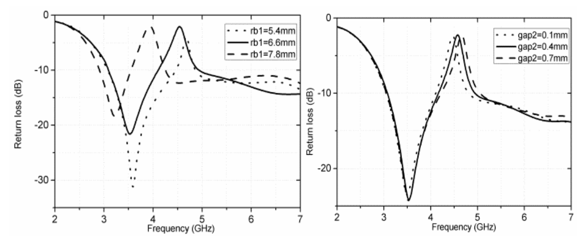

(a) (b)

Fig. 7. Simulation results for different parameters, (a) S_{11} for parameter *rb1* and (b) S_{11} for parameter *gap2*.

B. The outer split ring inserting

After getting the higher band-notched (3.8 GHz – 4.9 GHz) antenna, the outer split ring (*Ra*) embedded into the antenna is analyzed. The lower WLAN band (at 2.44 GHz) is obtained after embedding the *Ra*, while the band (2.5 GHz – 3.05 GHz) is notched. The length of *Ra* slot is determined by *Lsb* = 32 mm (about half of the guided wavelength ($\lambda_g/2$) calculated at 2.68 GHz).

Figure 8 illustrated the effects of the parameters *ra* and *wa*. From the figure, it is observed that the notched band shifts to lower frequency as *ra* increases, while the impedance matching of the antenna is improved as *wa* reduce. The current distribution at 2.68 GHz (notched frequency) and 2.44 GHz (resonant frequency) is given in Fig. 9, it can be seen that the current manly distributed around the *Ra* at the notched frequency 2.68 GHz.

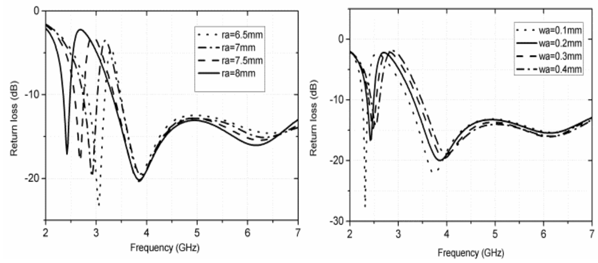

(a) (b)

Fig. 8. Simulation results for different parameters, (a) S_{11} for parameter *ra* and (b) S_{11} for parameter *wa*.

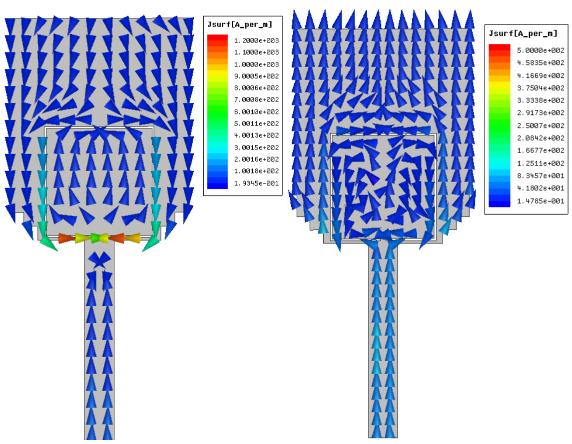

(a) (b)

Fig. 9. Simulated surface current distribution at 2.68 GHz, and 2.44 GHz; (a) 2.68 GHz and (b) 2.44 GHz.

III. RESULTS AND DISCUSSION

A triple band antenna prototype is fabricated on low cost FR4 ($\varepsilon_r = 4.4$, tan $\delta = 0.02$) substrate. We use Rohde and Schwarz ZVB 20 vector network analyzer to measure return-loss of the proposed antenna. The antenna with Rohde and Schwarz ZVB 20 vector network analyzer is shown in Fig. 10. The simulated and measured return-loss (S_{11}) characteristics of the proposed antenna obtained using HFSS 13.0 and the Rohde and Schwarz ZVB 20 vector network analyzer is shown in Fig. 11. From the measured results, three relative impedance bandwidths with -10 dB return loss are about 3.7 % (2.39 GHz – 2.48 GHz), 20.8% (3 GHz – 3.7 GHz), and 30% (5 GHz – 7 GHz), respectively, which show good agreement with the simulated results. The differences between the simulation and measurements could be due to the SMA connector and the manufacturing limits.

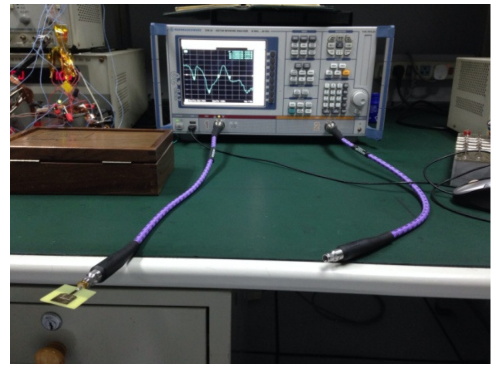

Fig. 10. Photograph of proposed triple band antenna with Rohde and Schwarz ZVB 20 vector network analyzer.

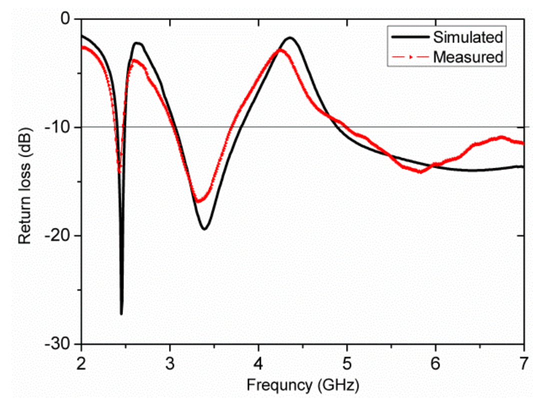

Fig. 11. Simulated and measured S_{11} for proposed triple band antenna.

The radiation patterns of the proposed antenna were measured in an anechoic chamber at UESTC with SATIMO antenna measurement system as shown in Fig. 12. The measured far-field radiation patterns of the proposed triple band antenna in the E-plane (*xz*-plane) and H-plane (*yz*-plane) at 2.44 GHz, 3.5 GHz, and 5.5 GHz are plotted in Fig. 13. It can be seen that the antenna behaves quite similarly to the typical printed monopoles. The H-plane patterns are almost omni-directional, while the E-plane patterns exhibit dipole-like behaviors at these frequencies. The measured peak gain from 2 GHz to 7 GHz is plotted in Fig. 14. As expected, the antenna gain exhibits two significant decreases at 2.7 GHz and 4.6 GHz, thus clearly indicating the effect of notched bands.

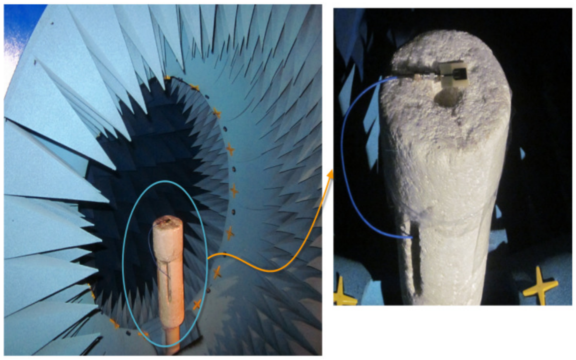

Fig. 12. Photograph of proposed triple band antenna in an anechoic chamber.

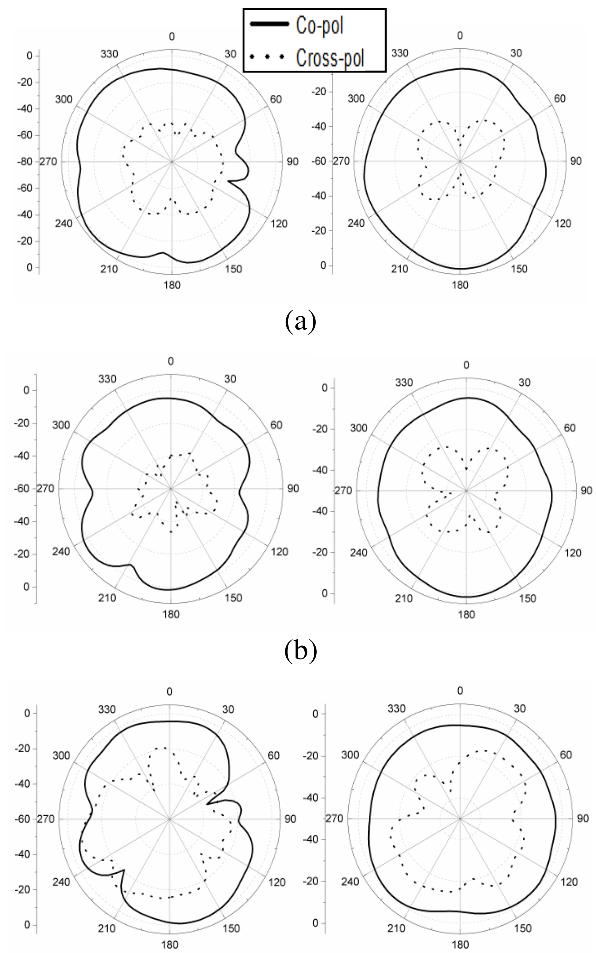

(a)

(b)

(c)

xz- plane yz-plane

Fig. 13. Measured radiation patterns of the proposed antenna; (a) 2.44 GHz, (b) 3.5 GHz, and (c) 5.5 GHz.

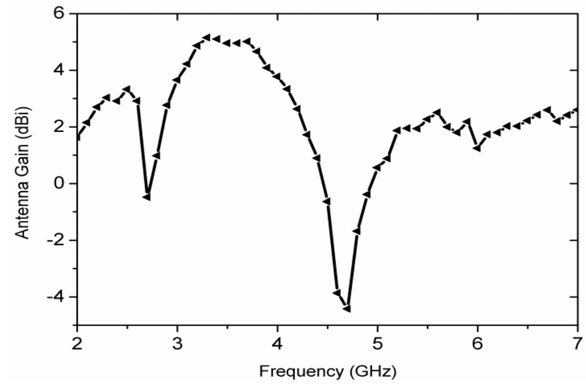

Fig. 14. Measured peak gain of the proposed antenna.

IV. CONCLUSION

A compact triple band antenna in simple structure for WLAN/WiMAX is proposed. This antenna consists of a regular microstrip-fed rectangle printed monopole antenna and a rectangle ground plane without slots. By embedding complementary split ring in the radiation element for band-rejected design, which does not increase the dimensions of the initial antenna, the triple band antenna is obtained. The measured results show that the impedance bandwidths range from 2.39 GHz – 2.48 GHz, 3 GHz – 3.7 GHz, and 5 GHz – 7 GHz, good performance for the WLAN (2.4/5.2/5.8) and WiMAX (3.5/5.5) bands. In addition, the proposed antenna has good radiation patterns and gains in the three operating bands. So this simple structure antenna is excellent candidate for wireless communications.

ACKNOWLEDGMENT

This work was supported by the National Natural Science Foundation of China (No.61172115 and No.60872029), the High-Tech Research and Development Program of China (No.2008AA01Z206), the Aeronautics Foundation of China (No.20100180003), and the Fundamental Research Funds for the Central Universities (No.ZYGX2009J037).

REFERENCES

[1] Y.-C. Chen, et al., “A compact triple-band planar monopole antenna for WLAN and WiMAX applications,” *Antenna Technology (IWAT), International Workshop*, pp. 311-314, 2013.

[2] J. Y. Jan and L. C. Tseng, “Small planar monopole antenna with a shorted parasitic inverted-L wire for wireless communications in the 2.4-, 5.2-, and 5.8-GHz bands,” *IEEE Trans. Antennas Propag.*, vol. 52, pp. 1903-1905, 2004.

[3] C. Y. Pan, C. H. Huang, and T. S. Horng, “Printed crisscross monopole antenna with a square con ductor-backed parasitic plane for dual-band WLAN applications,” *Microw. Opt. Technol. Lett.*, vol. 46, pp. 541-543, 2005.

[4] A. A. Ibrahim, A. E. Safwat, and H. El-Hennawy, “Triple-band microstrip-fed monopole antenna loaded with CRLH unit cell,” *IEEE Antennas Wirel. Propag. Lett.*, vol. 10, pp. 1547-1550, 2011.

[5] D. L. Jin, J. S. Hong, and H. Xiong, “Dual wideband antenna for WLAN/WiMAX and satellite system applications based on a metamaterial transmission line,” *Chin. Phys. Lett.*, vol. 29, no. 10, pp. 104101-104101-3, Oct. 2012.

[6] K. L. Sheeja, P. K. Sahu, S. K. Behera, and N. Dakhli, “Compact tri-band metamaterial antenna for wireless applications,” *Applied Computational Electromagnetics Society (ACES) Journal*, vol. 27, pp. 947-955, 2009.

[7] A. Almutairi, N. A. Aljuhaishi, and S. F. Mahmoud, “New compact and broadband patch antenna configurations for wireless applications,” *Applied Computational Electromagnetics Society (ACES) Journal*, vol. 24, pp. 437-445, 2009.

[8] X. Li, Y. F. Wang, X. W. Shi, W. Hu, and L. Chen, “Compact triple-band antenna with rectangular ring for WLAN and WiMAX applications,” *Microw. Opt. Technol. Lett.*, vol. 54, pp. 286-289, 2012.

[9] D. D. Krishna, M. Gopikrishna, and C. K. Aanandan, “A CPW-fed triple band monopole antenna for WiMAX/WLAN applications,” *Microwave Conference, EuMC 38th European*, pp. 897-900, 2008.

[10] M. C. Tang, S. Xiao, T. Deng, D. Wang, J. Guan, B. Wang, and G. D. Ge, “Compact UWB antenna with multiple band-notches for WiMAX and WLAN,” *IEEE Trans. Antennas Propag.*, vol. 59, pp. 1372-1376, 2011.

[11] Y. L. Kuo and K. L. Wong, “Printed double-T monopole antenna for 2.4/5.2 GHz dual-band WLAN operations,” *IEEE Trans. Antennas Propag.*, vol. 51, no. 9, pp. 2187-2192, 2003.

[12] K. G. Thomas and M. Sreenivasan, “Compact triple band antenna for WLAN/WiMAX applications,” *Electron. Lett.*, vol. 45, pp. 811-812, 2009.

[13] L. Bing, J. S. Hong, and B. Z. Wang, “A novel circular disc monopole antenna for dual-band WLAN applications,” *Applied Computational Electromagnetics Society(ACES) Journal*, vol. 27, pp. 41-448, 2012.

[14] P. Wang, G. J. Wen, and Y. J. Huang, “Compact CPW-fed planar monopole antenna with triple-band operation for WLAN/WiMAX applications,” *Applied Computational Electromagnetics Society (ACES) Journal*, vol. 27, pp. 691-696, 2012.

[15] C. N. Chiu and H. R. Chen, “A compact and wideband balance-fed triangular-monopole antenna for DCS/PCS/UMTS/WLAN/WiMAX applications,” *Microw. Opt. Technol. Lett.*, vol. 50, pp. 971-974, 2008.

[16] J. H. Lu and H. M. Chin, “Planar compact U-shaped patch antenna with high-gain operation for Wi-Fi/WiMAX application,” *Applied Computational Electromagnetics Society (ACES) Journal*, vol. 26, pp. 82-86, 2011.

[17] J. Y. Sze, C. I. G. Hsu, and J. J. Jiao, “CPW-fed circular slot antenna with slit back-patch for 2.4/5 GHz dual-band operation,” *Electron. Lett.*, vol. 42, pp. 563-564, 2006.

[18] R. L. Li, T. Wu, and M. M. Tentzeris, “A triple-band unidirectional coplanar antenna for 2.4/3.5/5-GHz WLAN/WiMax applications,” *IEEE International Symposium on Antennas & Propagation & USNC/URSI National Radio Science Meeting*, USA, June, 2009.

[19] S. Chaimool and K. L. Chung, “CPW-fed mirrored-L monopole antenna with distinct triple bands for WiFi and WiMAX applications,” *Electron. Lett.*, vol. 45, pp. 928-U17, 2009.

[20] W. J. Lui, C. H. Cheng, and H. B. Zhu, “Improved frequency notched ultrawideband slot antenna using square ring resonator,” *IEEE Trans. Antennas Propag.*, vol. 55, pp. 2445-2450, 2007.

[21] J. H. Jung, W. Choi, and J. Choi, “A small wideband microstrip-fed monopole antenna,” *IEEE Microw. Component Lett.*, vol. 15, 10, pp. 703-705, 2005.

[22] S. W. Su, K. L. Wong, and C. L. Tang, “Ultra-wideband square planar monopole antenna for ieee 802.16a operation in the 2-11-GHz band,” *Microw. Opt. Technol. Lett.*, vol. 42, pp. 463-466, 2004.

[23] W. Jiang and W. Che, “A novel UWB antenna with dual notched bands for WiMAX and WLAN applications,” *IEEE Antennas Wirel. Propag. Lett.*, vol. 11, pp. 293-296, 2012.

Da-lin Jin was born in Sichuan, China. She received her B.S. degree in Electronics Information Science and Technology from Chengdu University of Information Technology in 2010. She is a graduate student major in Radio Physics in the University of Electronic Science and Technology of China now.

Her research interests include left-handed metamaterials technology and the applications of antenna with metamaterials.

Ting-ting Bu was born in Guizhou, China. She received her B.S. degree in University of Electronic Science and Technology of China in 2008. She is a master in Electronics and Communications Engineering of the University of Electronic Science and Technology of China now. Her research interests is antenna technology.

Jing-song Hong received the B.Sc. degree in electromagnetics from Lanzhou University, China, in 1991, and the M.Sc. and Ph. D. degrees in electrical engineering from the University of Electronic Science and Technology of China (UESTC), in 2000 and 2005, respectively. He is now a professor with UESTC. From 1991 to 1993, he was a Circuit Designer with the Jingjiang Radar Factory, Chengdu, China. From 1993 to 1997, he was a Testing Engineer with SAE Magnetics (HK) Ltd, Guangdong, China. From 1999 to 2002, he was a Research Assistant with the City University of Hong Kong. His research interest includes the use of numerical techniques in electromagnetics and the use of microwave methods for materials characterization and processing.